Electronic Supplementary Material (ESI) for Inorganic Chemistry Frontiers.

Supporting Information

An Imidazole Derivative Based Chemodosimeter for Zn^{2+} and Cu^{2+} ions through "On-Off-On" Switching with Intracellular Zn^{2+} Detection

Shagufi N. Ansari[a], Anoop K. Saini[a], Pratibha Kumari[b] and Shaikh M. Mobin*[a,b,c]

[a]Discipline of Chemistry, [b]Discipline of Biosciences and Bio-Medical Engineering and [c]Discipline of Metallurgy Engineering and Materials Science, Indian Institute of Technology Indore, Simrol, Khandwa Road, Indore 453552, India.

*Email: xray@iiti.ac.in

Tel: +91 731 2438 752

Experimental details

The common reagents and solvents were purchased from Merck and S. D. Fine Chem. Ltd. Solvents were distilled following the standard literature methods prior to their use. O-Vanillin, MTT and 1-(3-Aminopropyl)Imidazole were procured from Sigma Aldrich Chemical Co., USA. Dulbecco's modified eagle medium (DMEM) were procured from Gibco. DU145 (prostate cancer) and HeLa cells (cervical cancer cell line) cell lines were obtained from National Centre for Cell Science, Pune. India

Physical measurements

^{1}H NMR (400 MHz) and^{13}C NMR (100 MHz) spectra were recorded on a Bruker Avance (III) instrument by using DMSO-d6 and D_2O as a deuterated solvents. ^{1}H NMR chemical shifts are reported in parts per million (ppm) relative to the solvent residual peak (DMSO-d6, 2.50 ppm) and ^{13}C NMR chemical shifts are reported relative to the solvent residual peak (DMSO-d6, 39.7 ppm). UV-vis spectroscopic measurements were performed on a Varian UV-vis spectrophotometer (model: Cary 100) using a quartz cuvette with a path length of 1 cm. fluorescence spectra were recorded on a Fluoro Max-4 spectrofluorometer and an excitation and emission slits were used 5/5 nm. The HRMS spectrum and life time measurement of **HL** was recorded on a Bruker-Daltonics, micrOTOF-QII mass spectrometer and TCSPC system from Horiba Yovin (model: Fluorocube-01-NL). The data analysis was performed using IBH DAS (version 6, HORIBA Scientific, Edison, NJ) decay analysis software.

Crystal structure determination of HL, 1 and 2

Single crystal X-ray data were collected at 293 K using graphite-monochromated Mo Kα (λα = 0.71073 Å) source. The approach for the data collection of **HL**, **1** and **2** were apparaised by using CrysAlisPro CCD software. The data were collected by using the standard phi-omega scan techniques and were scaled and reduced using CrysAlisPro RED software. The structures were solved by direct methods using SHELXS-2014.[1] The positions of all the atoms were obtained by

direct methods. All nonhydrogen atoms were refined anisotropically and remaining hydrogen atoms were placed in geometrically constrained positions and refined with isotropic temperature factors, generally 1.2 × Ueq of their parent atoms. Despite several attempts we were unable to generate better quality crystals for **2**. All the H-bonding, C–H···π interactions and molecular structure drawings were prepared using the program Mercury (ver 3.1) and Diamond (ver 3.1d).[2] The crystallographic refinement data are placed in **Table 1** and selected bond distances and bond angles are shown in **Table S1**.

Table S1: Hydrogen Bonding in **HL, 1** and **2 [**Å and (º)].

	D-H···A	d(D-H)	d(H···A)	d(D···A)	<(DHA)
HL					
1	C(13)-H(13)N···O(1)#(2)	0.930(.000)	2.642	3.537	161.72(0.04)
2	C(13)-H(13)N···O(2)#(2)	0.930(.000)	2.622	3.375	138.44(0.02)
Equivalent positions: x-1/2,-y+1/2,-z+1					
1					
3	C(20)H(20)N···O(3)#(2)	0.930(.004)	2.638(0.003)	3.515(0.005)	157.39(0.37)
Equivalent positions: -x+1,+y-1/2,-z+1/2+1					
2					
4	C(20)-H(20)N···O(3)#(2)	0.930(.013)	2.642(0.008)	3.496(0.015)	153.01(0.85)
Equivalent positions: -x+1,+y+1/2,-z+1/2					

Table S2: Selected bond distances (Å) of **1** and **2**

Bond Distances	**1**	**2**
Zn(1)-O(2)	2.011(3)	-
Zn(1)-O(3)	2.015(3)	-
Zn(1)-N(2)	2.096(3)	-
Zn(1)-N(1)	2.112(3)	-
Zn(1)-N(4)	2.087(3)	-
Cu(1)-O(2)	-	1.916(6)
Cu(1)-O(3)	-	1.906(6)
Cu(1)-N(2)	-	2.272(7)
Cu(1)-N(1)	-	2.030(7)
Cu(1)-N(4)	-	2.029(7)
Cu(1)-O(2)	-	1.916(6)

Table S3: Selected bond angles(º) of **1** and **2.**

Bond angles	**1**	
O(2)-Zn(1)-O(3)	175.76(11)	-
O(2)-Zn(1)-N(4)	92.20(13)	-
O(3)-Zn(1)-N(4)	88.90(12)	-
O(2)-Zn(1)-N(2)	94.06(13)	-
O(3)-Zn(1)-N(2)	89.19(12)	-
N(4)-Zn(1)-N(2)	114.81(13)	-
O(2)-Zn(1)-N(1)	87.37(12)	-
O(3)-Zn(1)-N(1)	89.04(12)	-
N(4)-Zn(1)-N(1)	137.04(13)	-
O(3)-Cu(1)-O(2)	-	176.2(3)
O(3)-Cu(1)-N(1)	-	88.0(4)
O(2)-Cu(1)-N(1)	-	90.2(3)
O(3)-Cu(1)-N(4)	-	90.8(3)
O(2)-Cu(1)-N(4)	-	91.5(3)
N(1)-Cu(1)-N(4)	-	147.3(3)
O(3)-Cu(1)-N(2)#1	-	87.4(3)
O(2)-Cu(1)-N(2)#1	-	89.8(3)
N(1)-Cu(1)-N(2)#1	-	104.1(3)
N(4)-Cu(1)-N(2)#1	-	108.5(3)

Table S4: Average Life time measurement of **1**.

τ_1	τ_2	α_1	α_2	χ^2	$<\tau>$
0.10 ns	9.73 ns	0.23	0.77	1.09	7.50 ns

Table S5: Photophysical properties of **HL** and **1** and **2**.

Compound[a]	$\lambda_{(S0\rightarrow S1)}$ (nm)	ε (M^{-1} cm^{-1})	λ_{em}[b] (nm)	Φ[c]
HL	265	6.1×10^4	-	-
	330	1.3×10^4	-	-
1	275	4.3×10^4	-	-
	380	1.2×10^4	470	0.520
2	276	7.1×10^4	-	-
	377	1.7×10^4	-	-

[a]Recorded in Acetonitrile. [b]Excited at $\lambda_{S0\rightarrow S1.}$ [c]Determined by using quinine sulfate as standard(Φ_{st}=0.54, 0.1 M H_2SO_4).

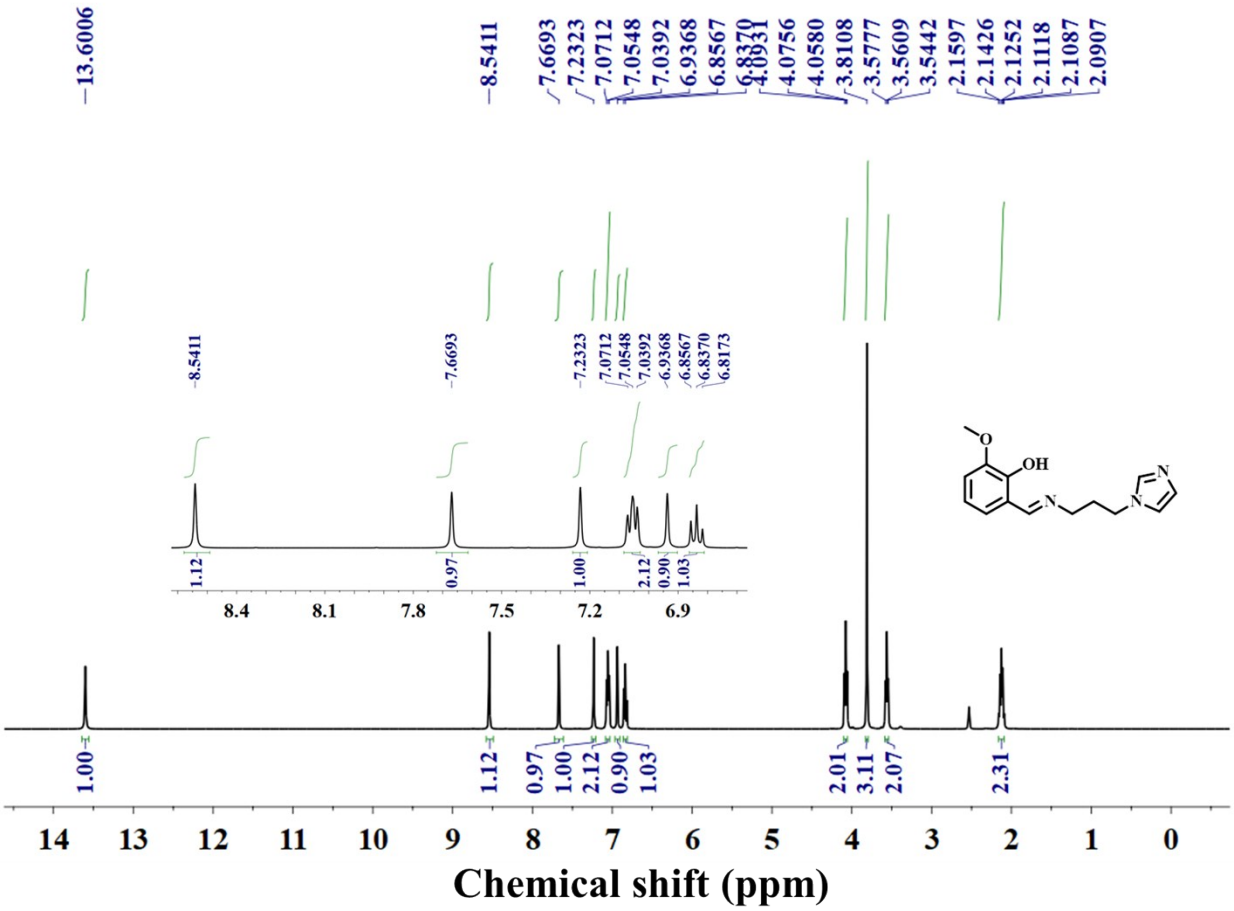

Fig S1. ^{1}H NMR spectrum of **HL**.

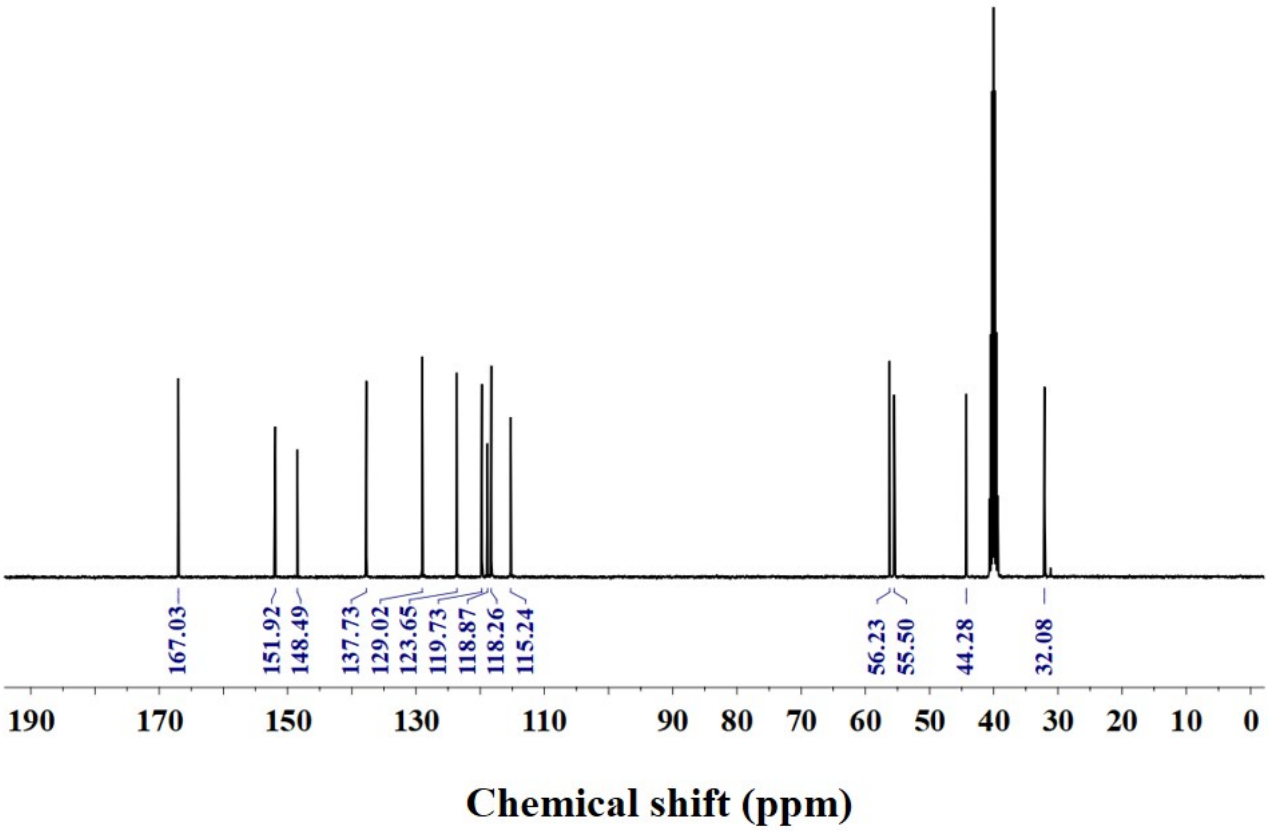

Fig S2. ^{13}C NMR spectrum of **HL**.

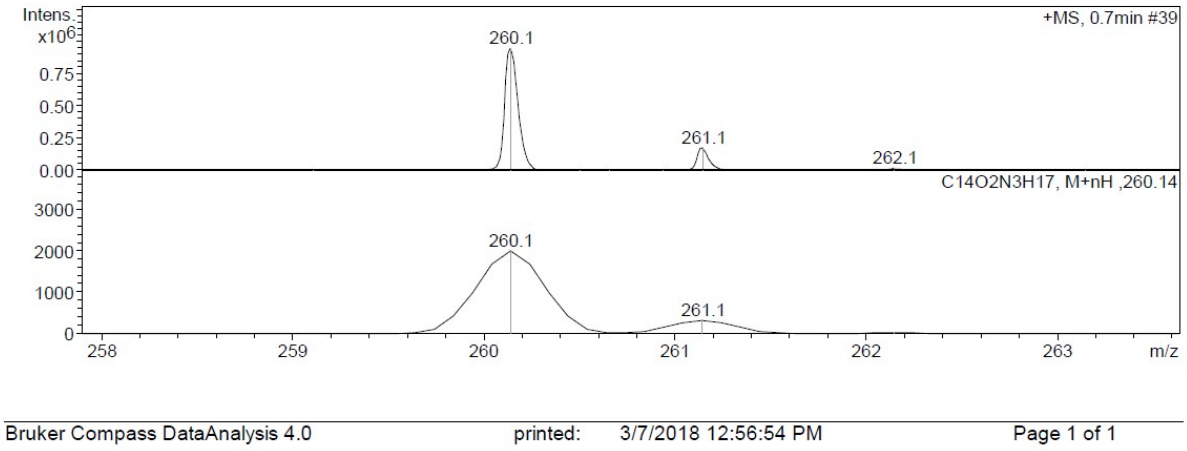

Fig S3. HRMS spectrum of **HL**.

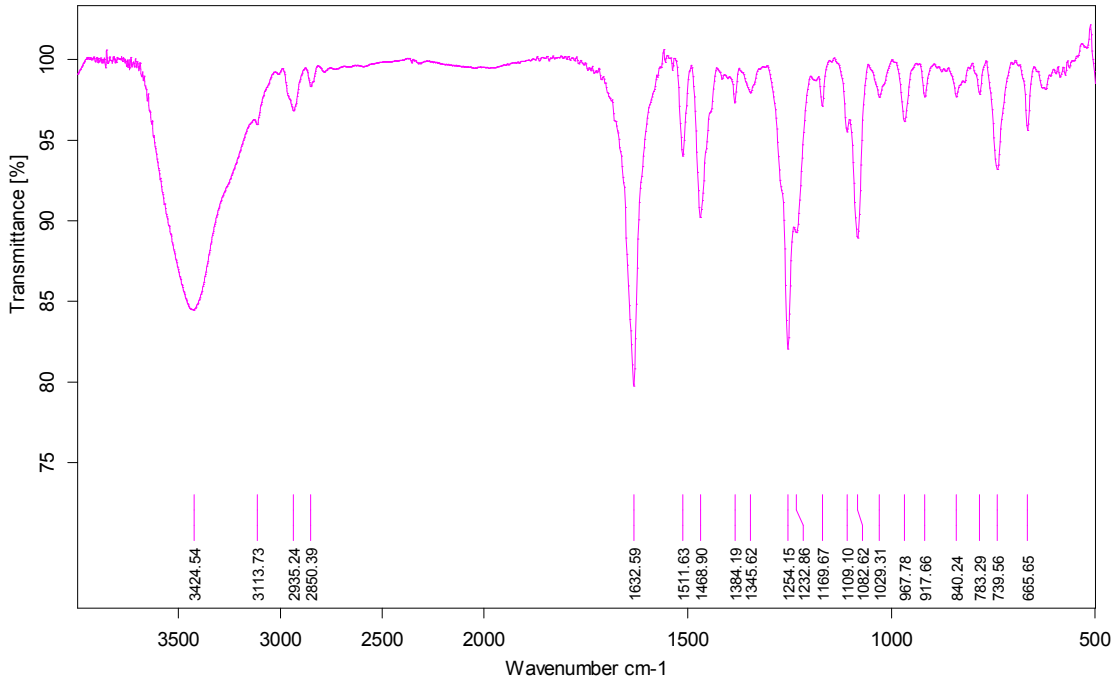

Fig S4. IR Spectrum of **HL**.

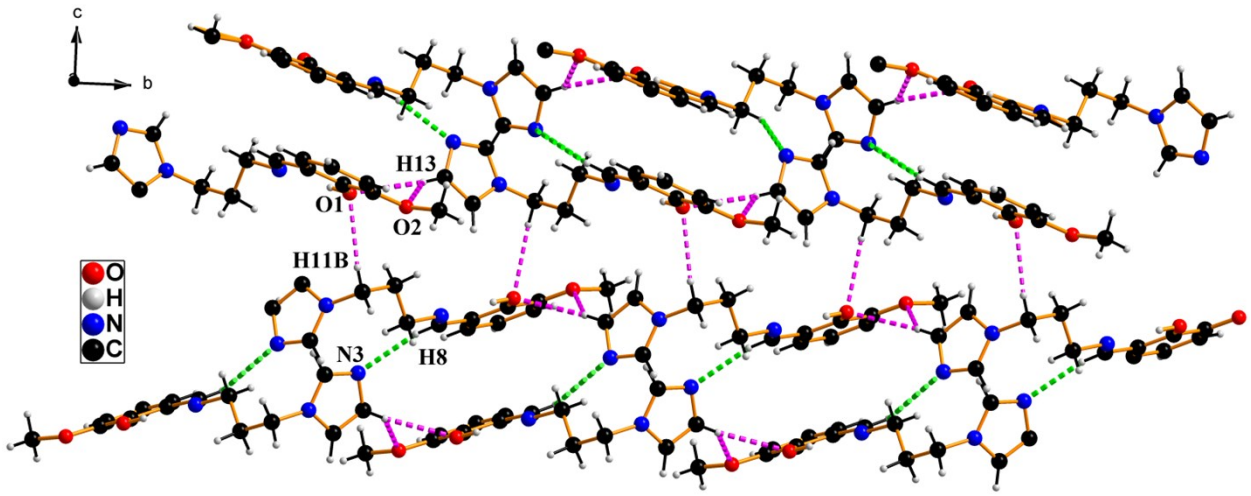

Fig S5. Packing diagram of **HL,** showing C-H···O and C-H···N, H-bonding interaction forming 1D and 2D network.

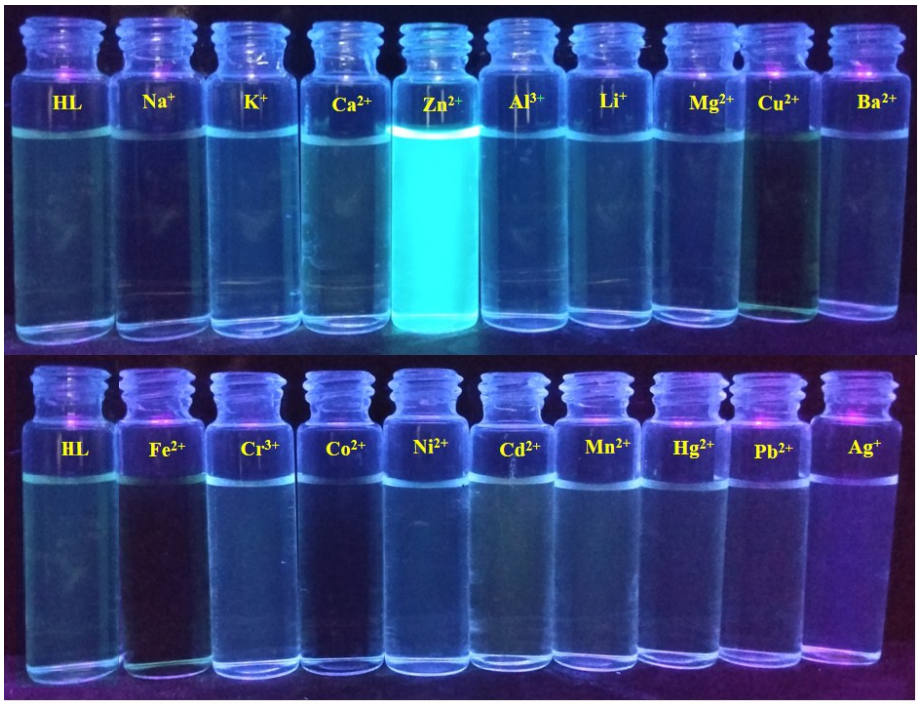

Fig S6. Colorimetric detection of $\mathbf{Zn^{2+}}$ using **HL** (10 equivalent of each metal ions with respect to $\mathbf{L_1}$).

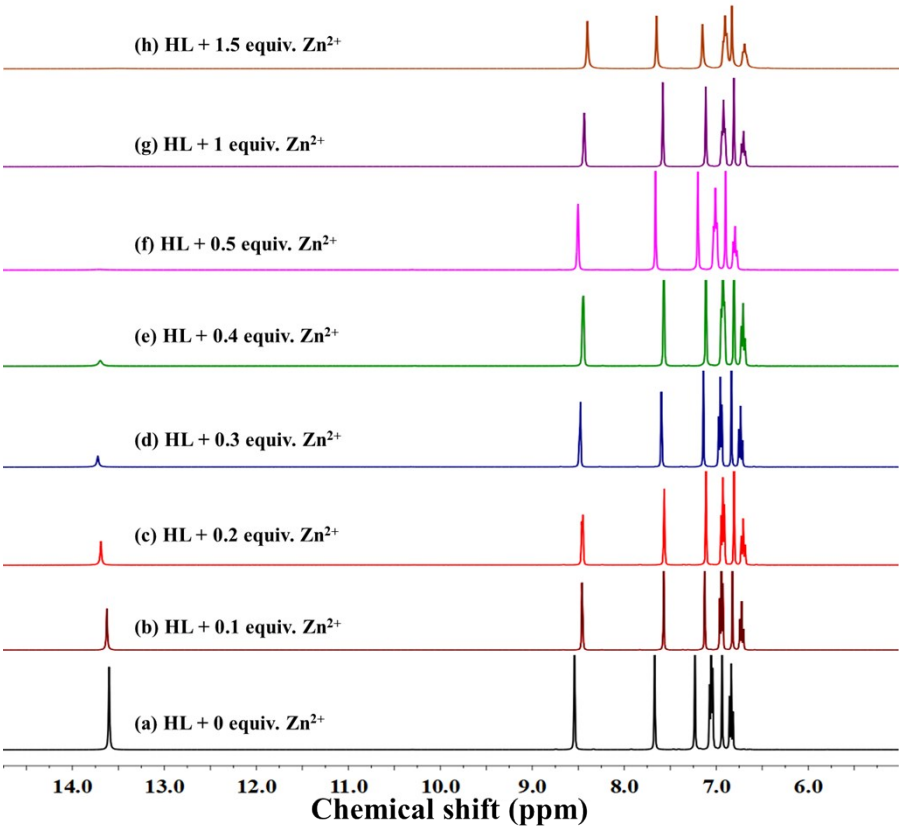

Fig S7. ^{1}H NMR spectra of **HL** in DMSO-D6 at 25°C and the analogous changes after the continuous addition of different equivalents of $Zn(NO_3)_2 \cdot 6H_2O$ in D_2O from (a) **HL**, (b) **HL** + 0.1 equiv. Zn^{2+}, (c) **HL** + 0.2 equiv. Zn^{2+}, (d) **HL** + 0.3 equiv. Zn^{2+}, (e) **HL** + 0.4 equiv. Zn^{2+} and (f) **HL** + 0.5 equiv. Zn^{2+}

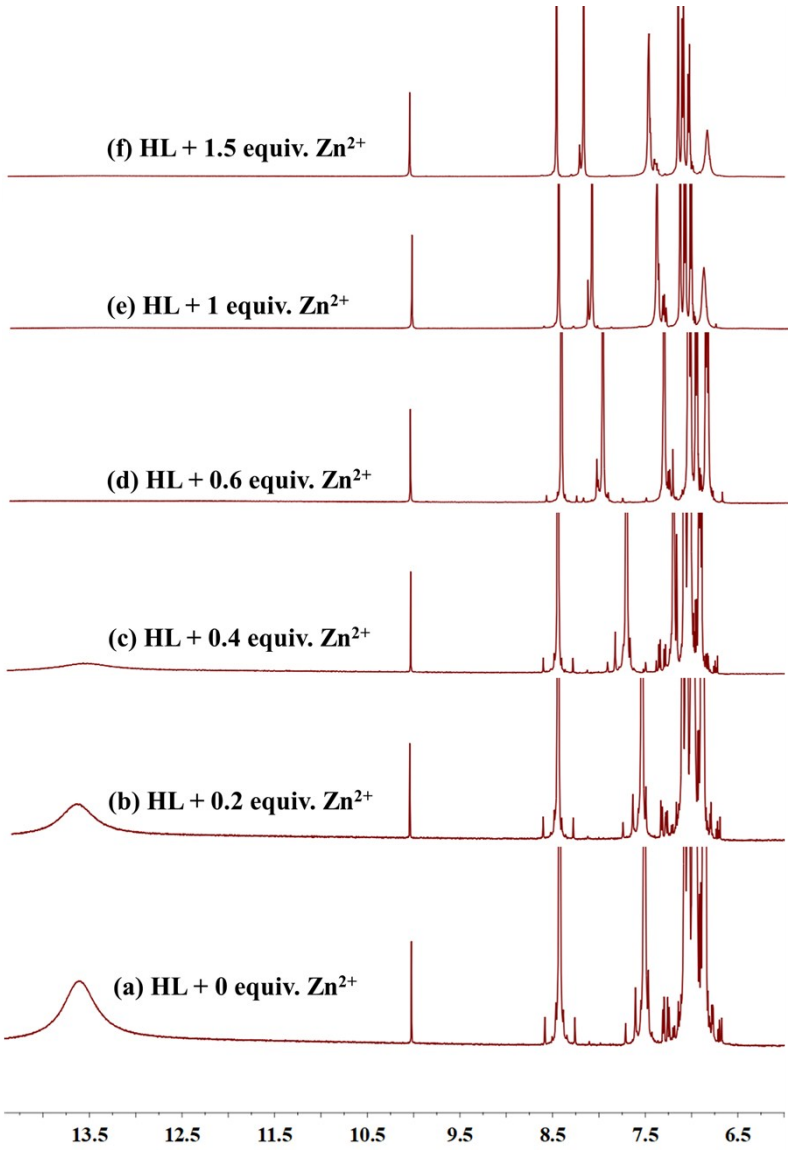

Fig S8. ^{1}H NMR spectra of **HL** in CD_3CN at 25°C and the analogous changes after the continuous addition of different equivalents of $Zn(NO_3)_2 \cdot 6H_2O$ in D_2O from (a) **HL**, (b) **HL** + 0.2 equiv. Zn^{2+}, (c) **HL** + 0.4 equiv. Zn^{2+}, (d) **HL** + 0.6 equiv. Zn^{2+}, (e) **HL** + 1 equiv. Zn^{2+} and (f) **HL** + 1.5 equiv. Zn^{2+}.

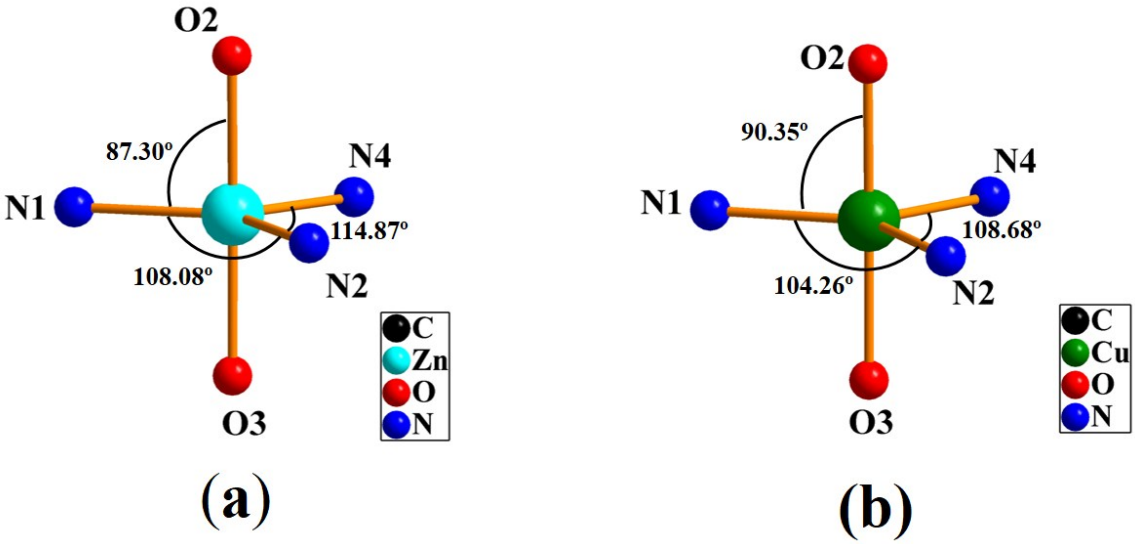

Fig S9. Ball and stick model showing penta-coordinated environment (distorted trigonal bipyramidal geometry) in **1(a)** and **2(b)**.

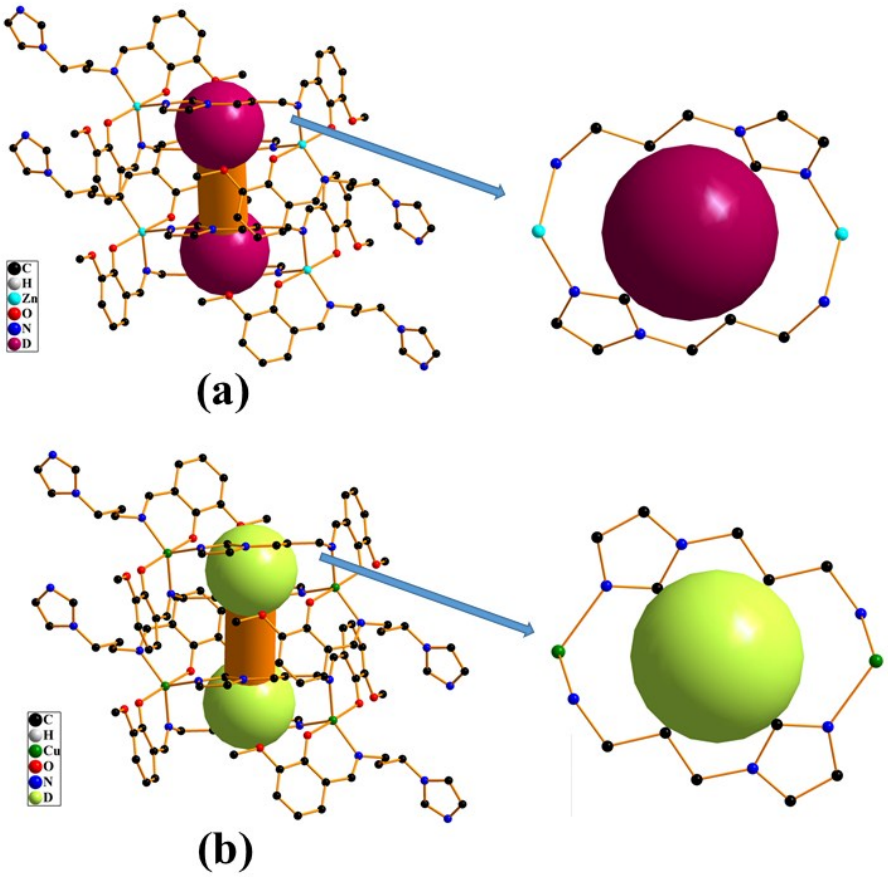

Fig S10. Cavity inside the metallacycle (a) in complex **1**, (b) in complex **2**.

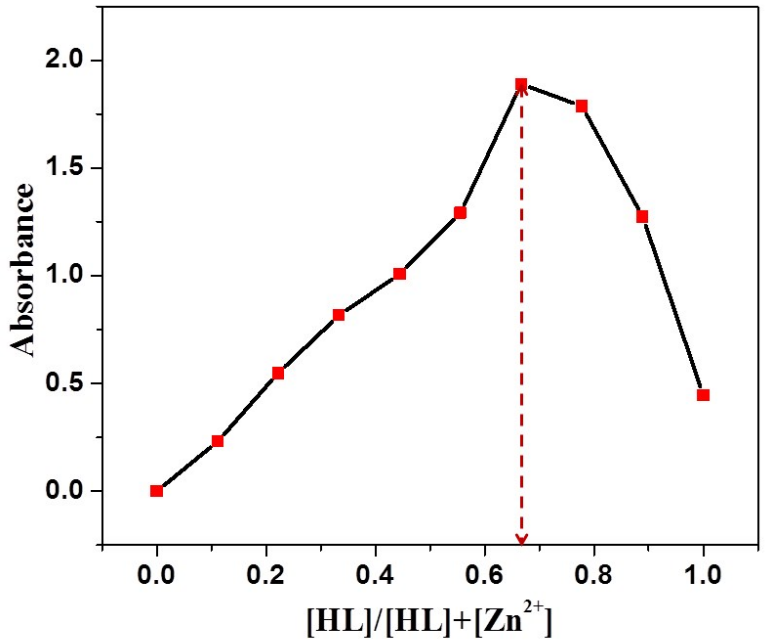

Fig S11. Job's plot showing Zn^{2+}:HL(1:2) complex recorded in CH_3CN-H_2O solution.

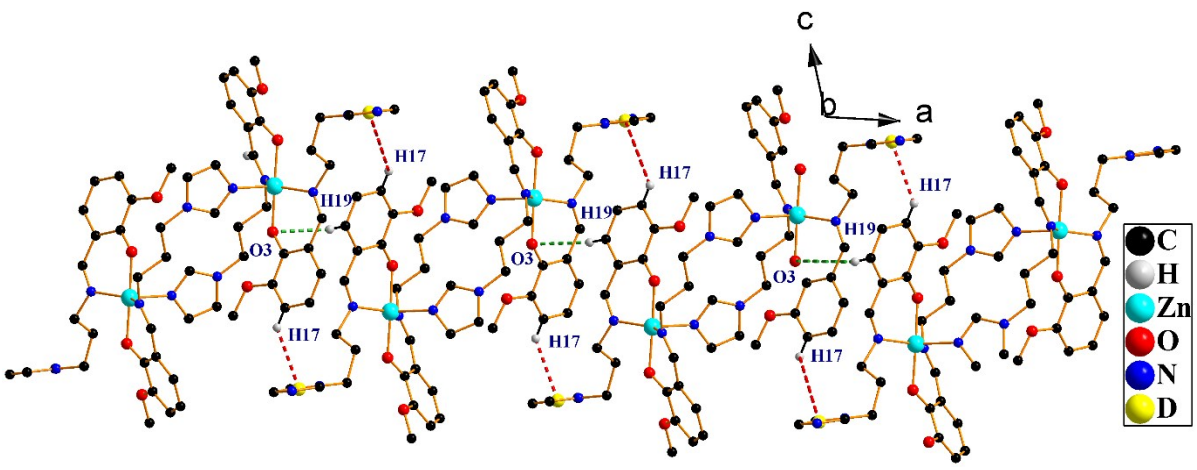

Fig S12. Packing diagram of intermolecular Hydrogen Bonding and C H···π interactions forming 1D layer in **1**, where D is the dummy atom.

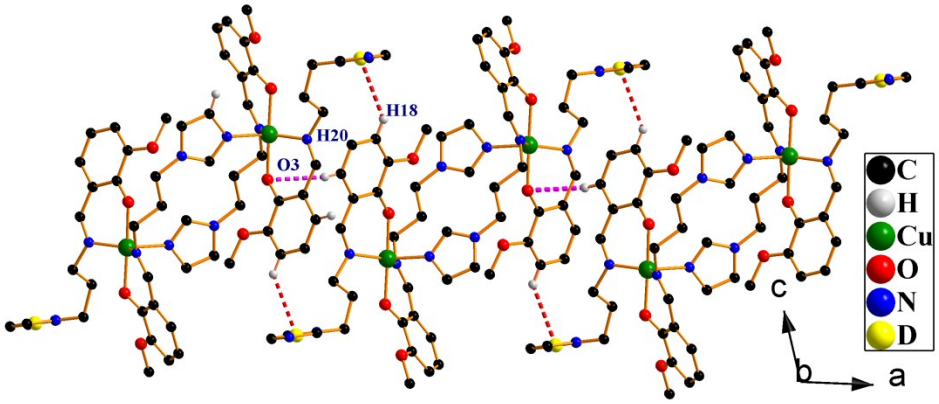

Fig S13. Packing diagram of intermolecular Hydrogen Bonding and C H···π interactions forming 1D layer in **2**, where D is the dummy atom.

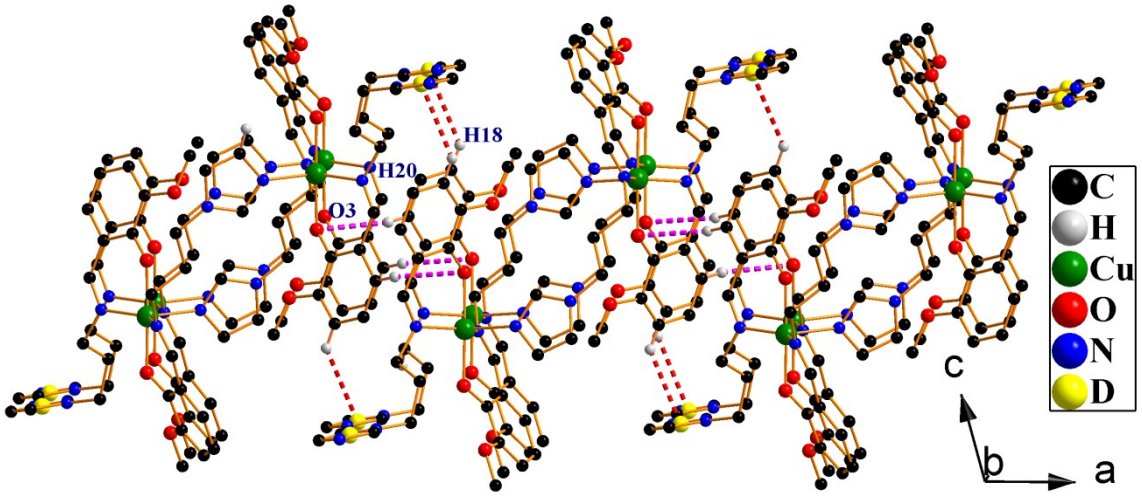

Fig S14. Packing diagram of intermolecular hydrogen bonding and C-H···π interactions in **2**. (Where D is the dummy atom).

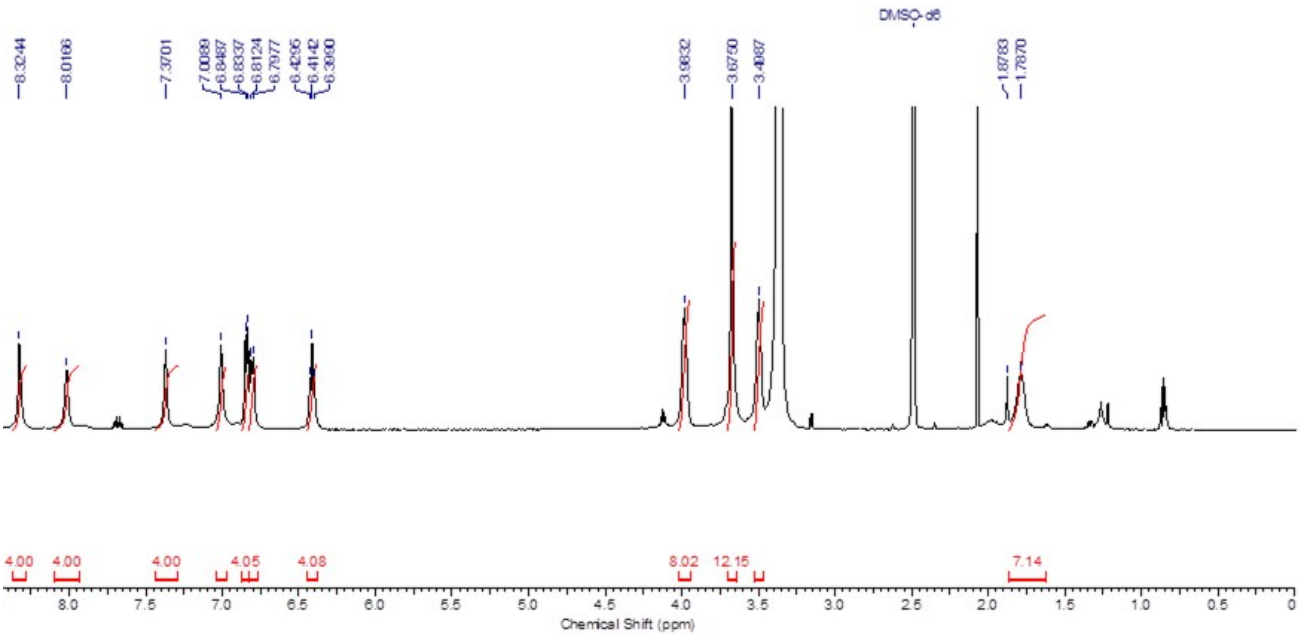

Fig S15. ^{1}H NMR spectrum of Complex **1**.

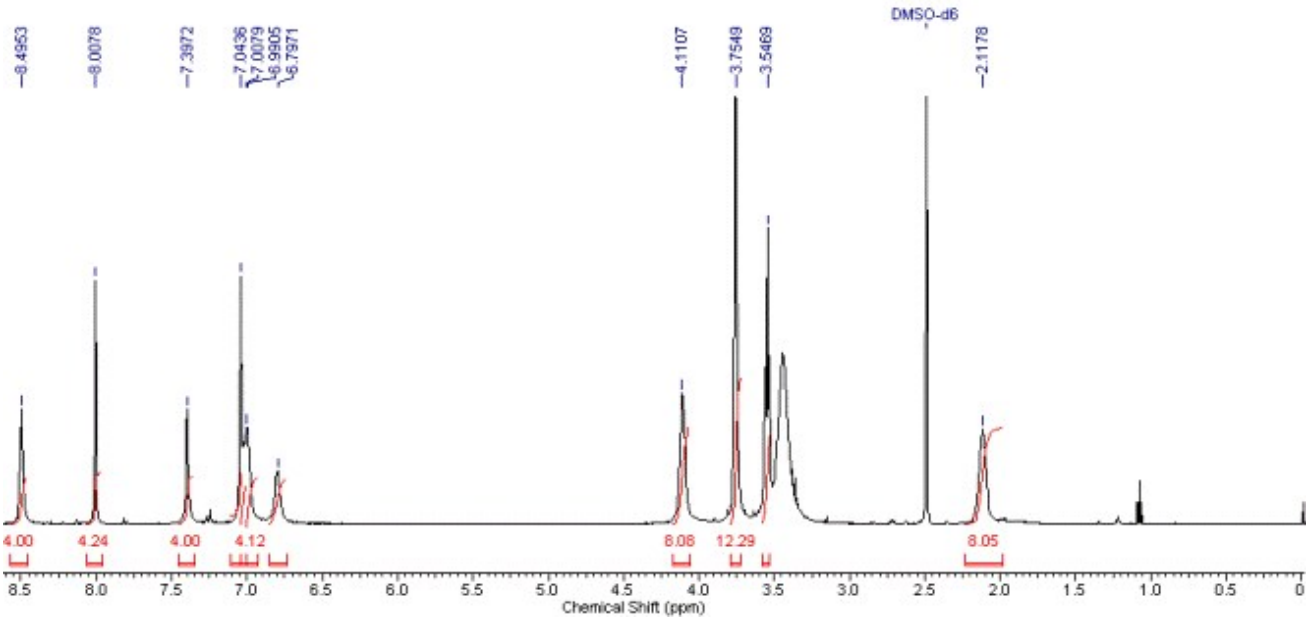

Fig S16. ^{1}H NMR spectrum of Complex **2**.

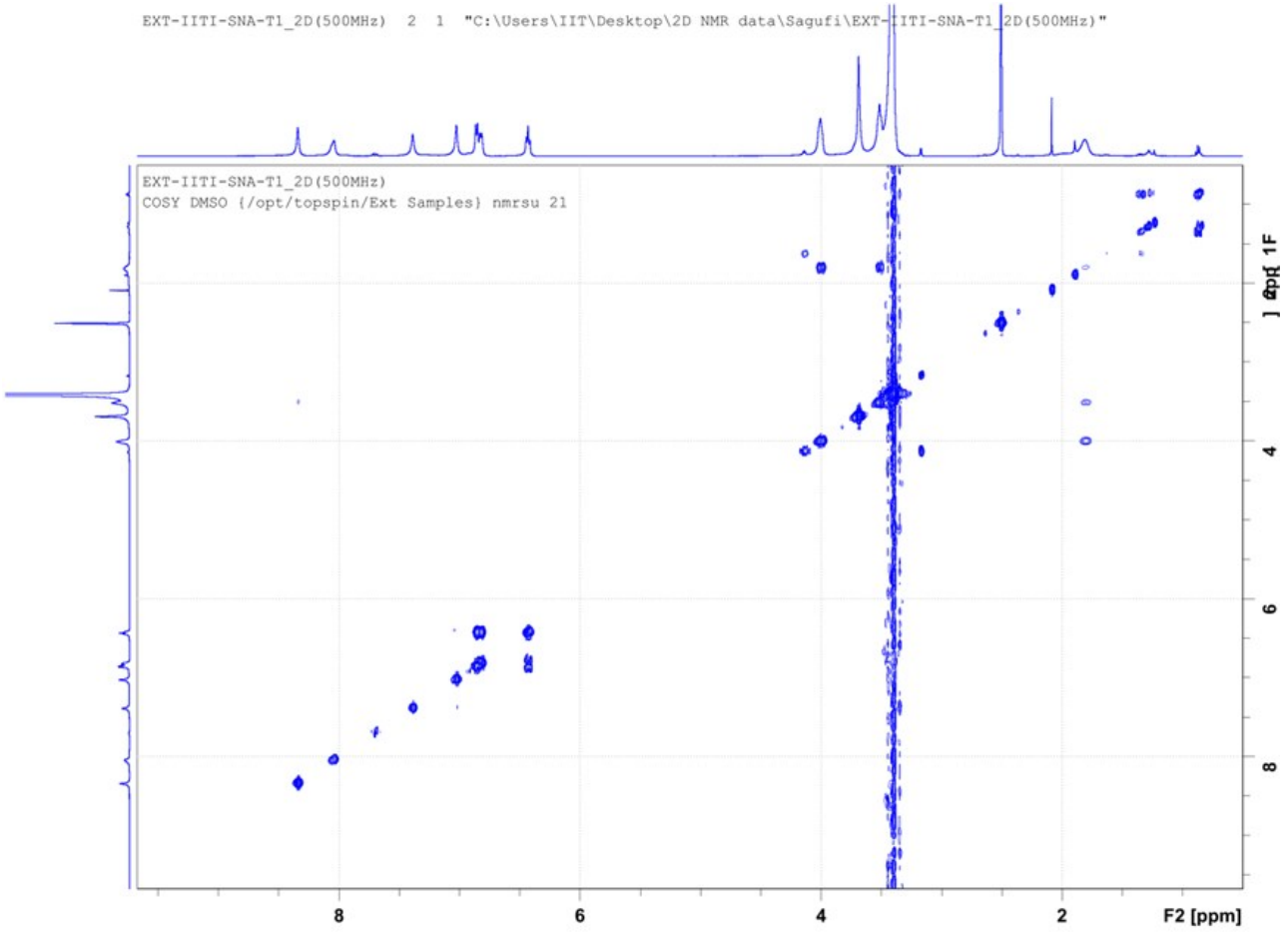

Fig S17. COSY (DMSO-*d*6, 500MHz) of Complex **1**.

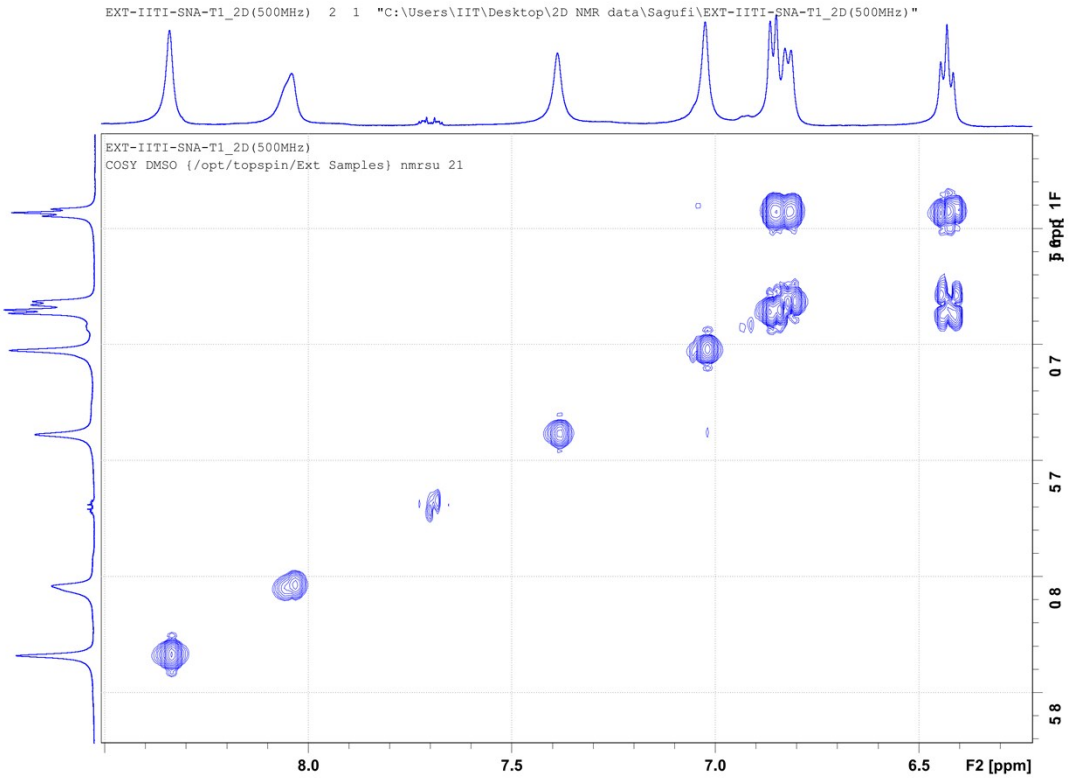

Fig S18. COSY (DMSO-*d*6, 500MHz) of Complex **1** (Aromatic region).

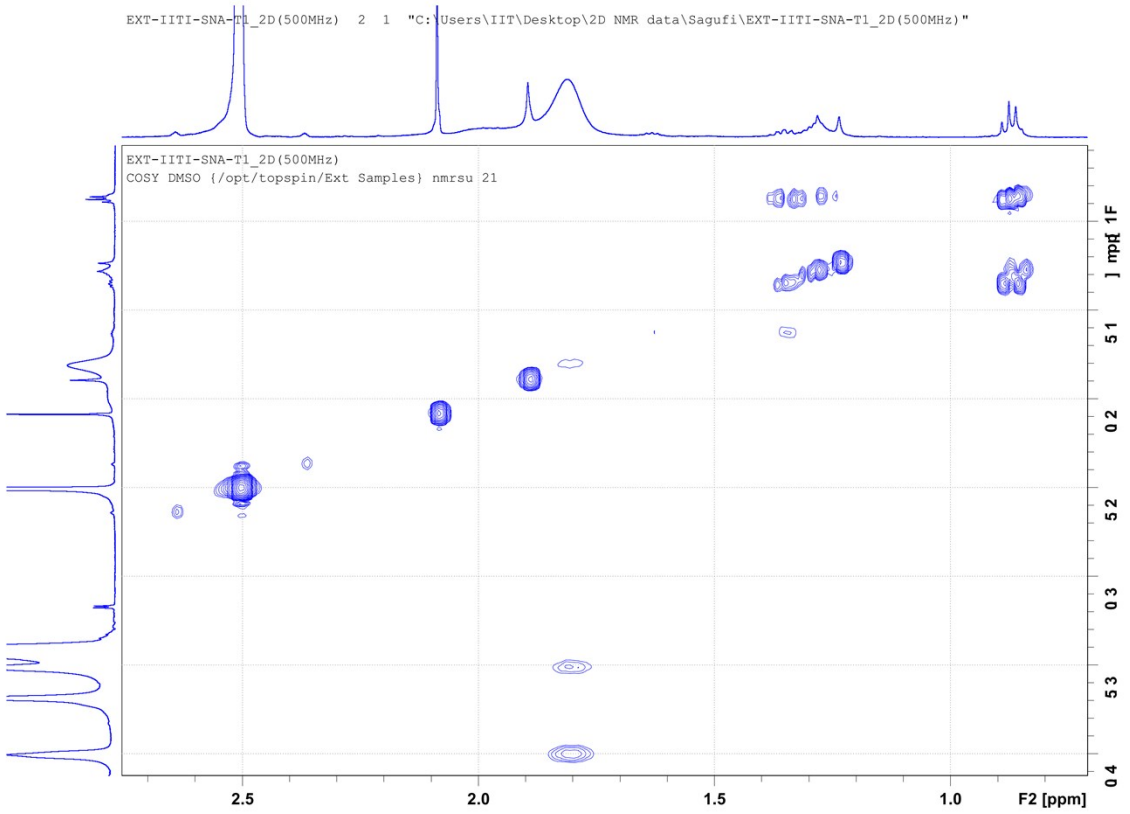

Fig S19. COSY (DMSO-*d*6, 500MHz) of Complex **1** (Aliphatic region).

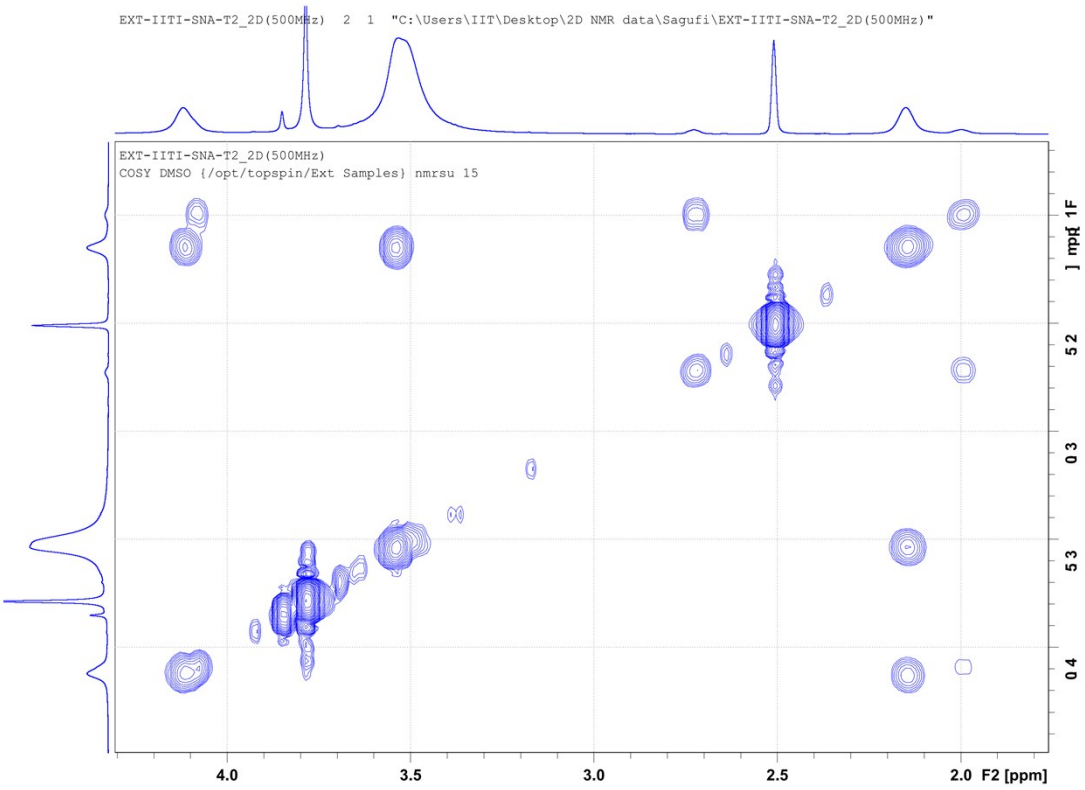

Fig S20. COSY (DMSO-*d*6, 500MHz) of Complex **2**.

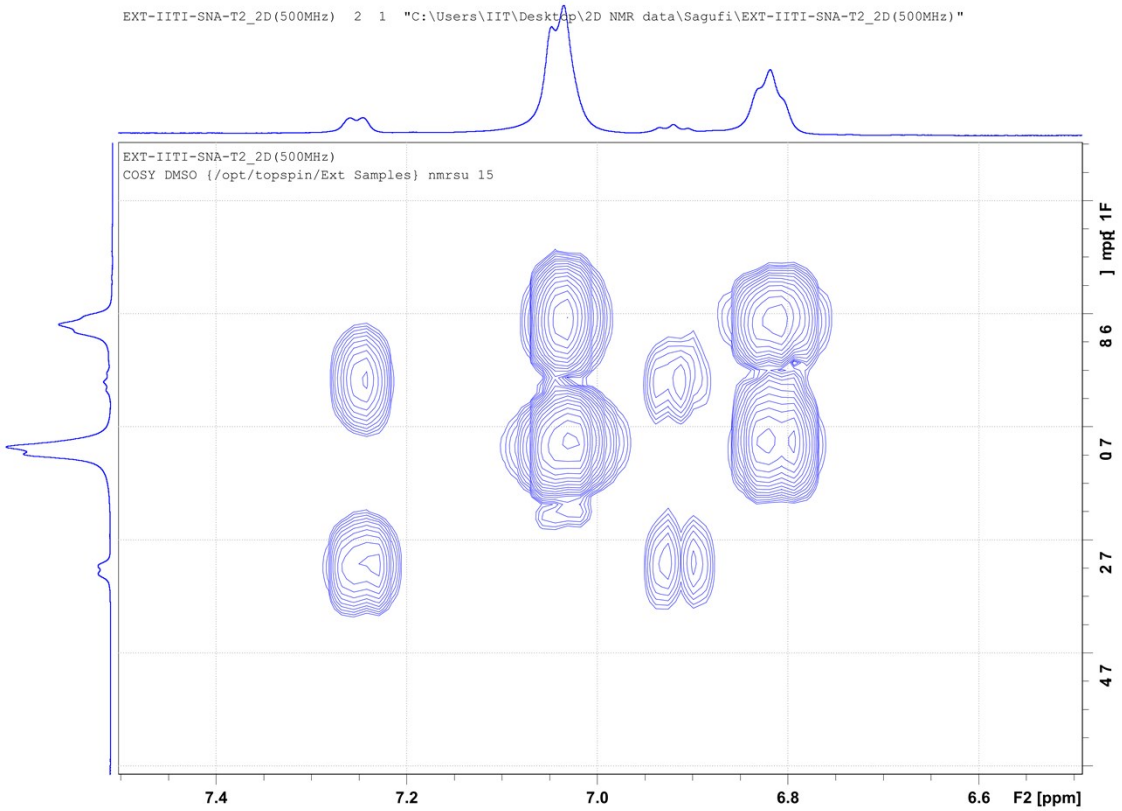

Fig S21. COSY (DMSO-*d*6, 500MHz) of Complex **2** (Aromatic region).

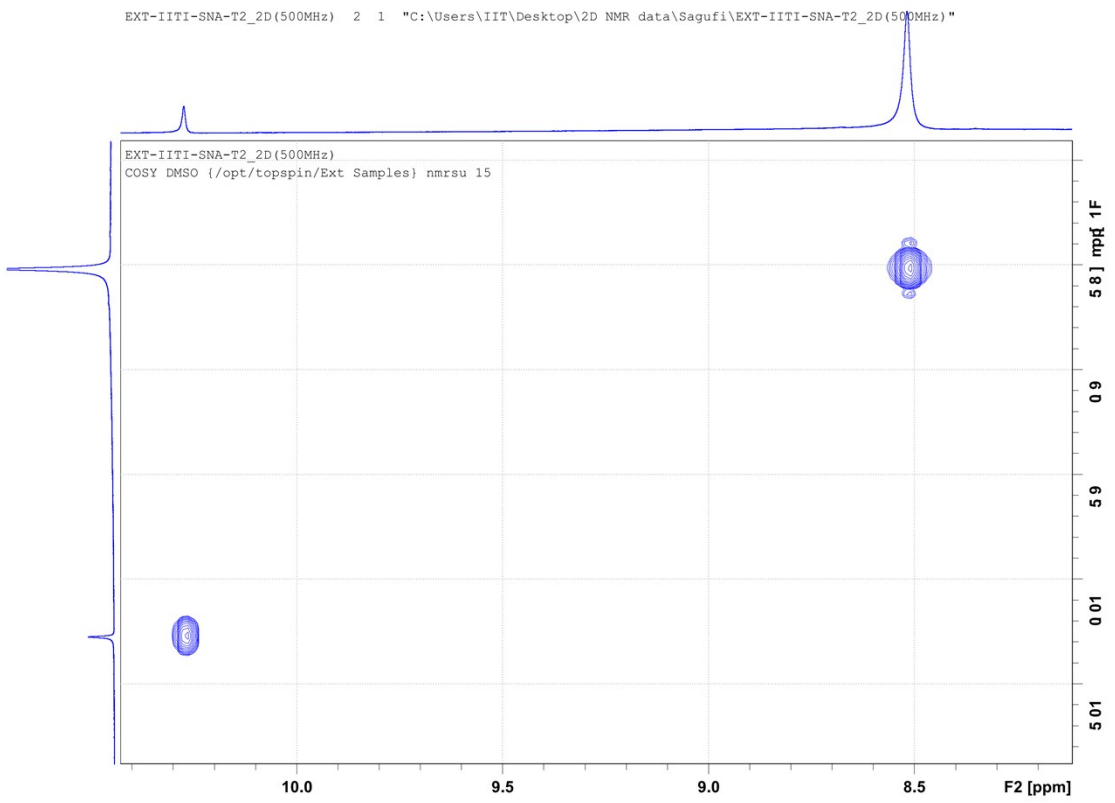

Fig S22. COSY (DMSO-*d*6, 500MHz) of Complex **2** (Aliphatic region).

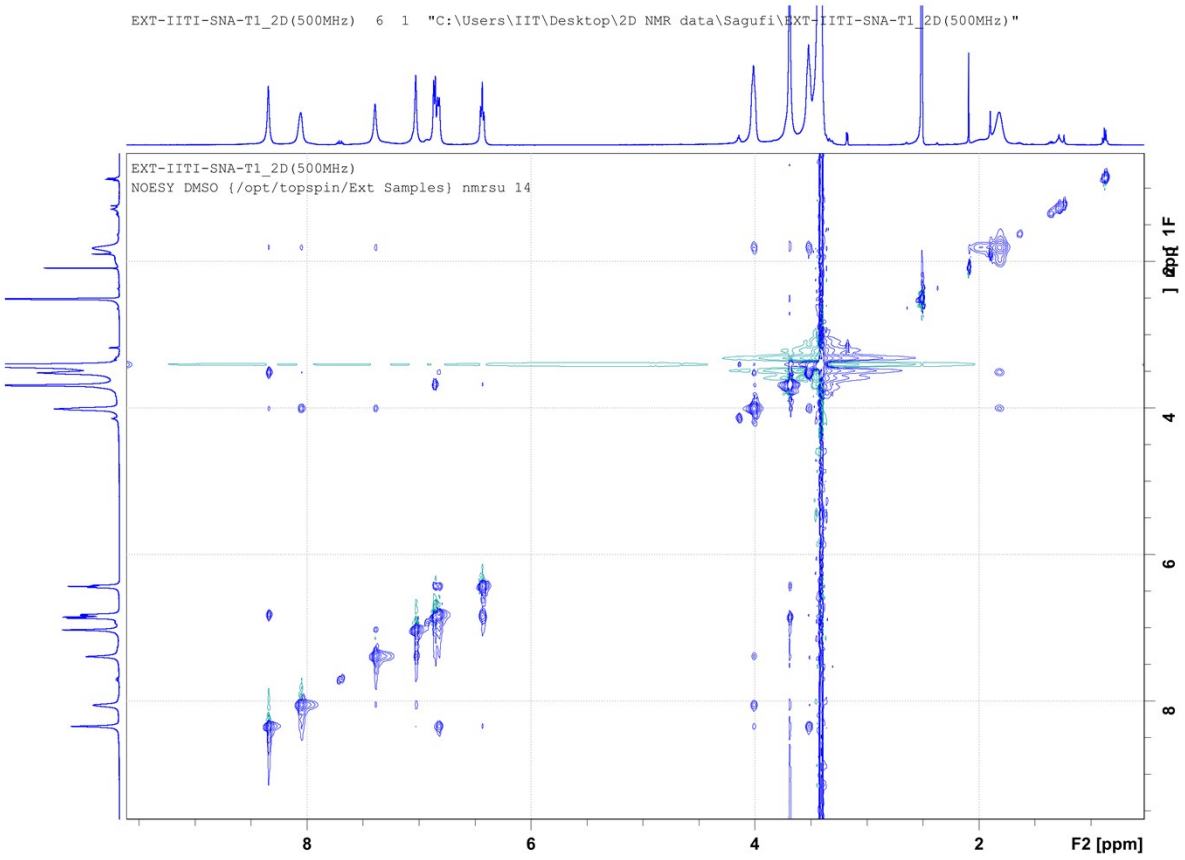

Fig S23. NOESY (DMSO-*d*6, 500MHz) of Complex **1**.

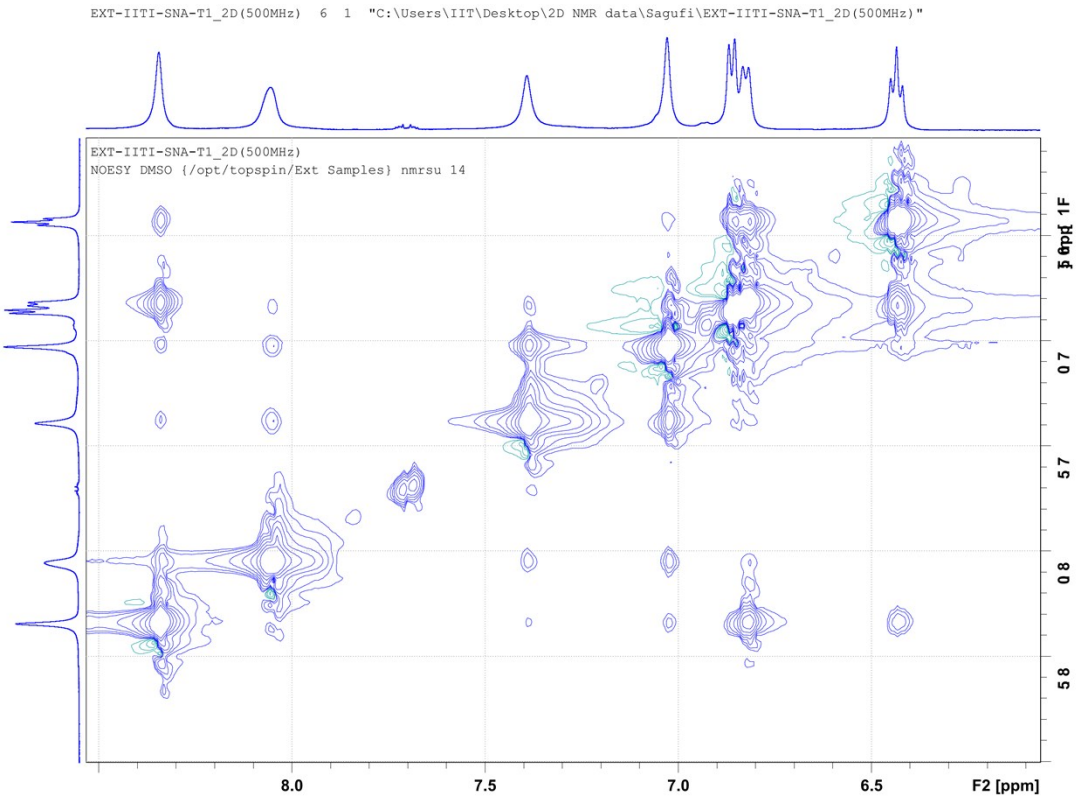

Fig S24. NOESY (DMSO-*d*6, 500MHz) of Complex **1** (Aromatic region).

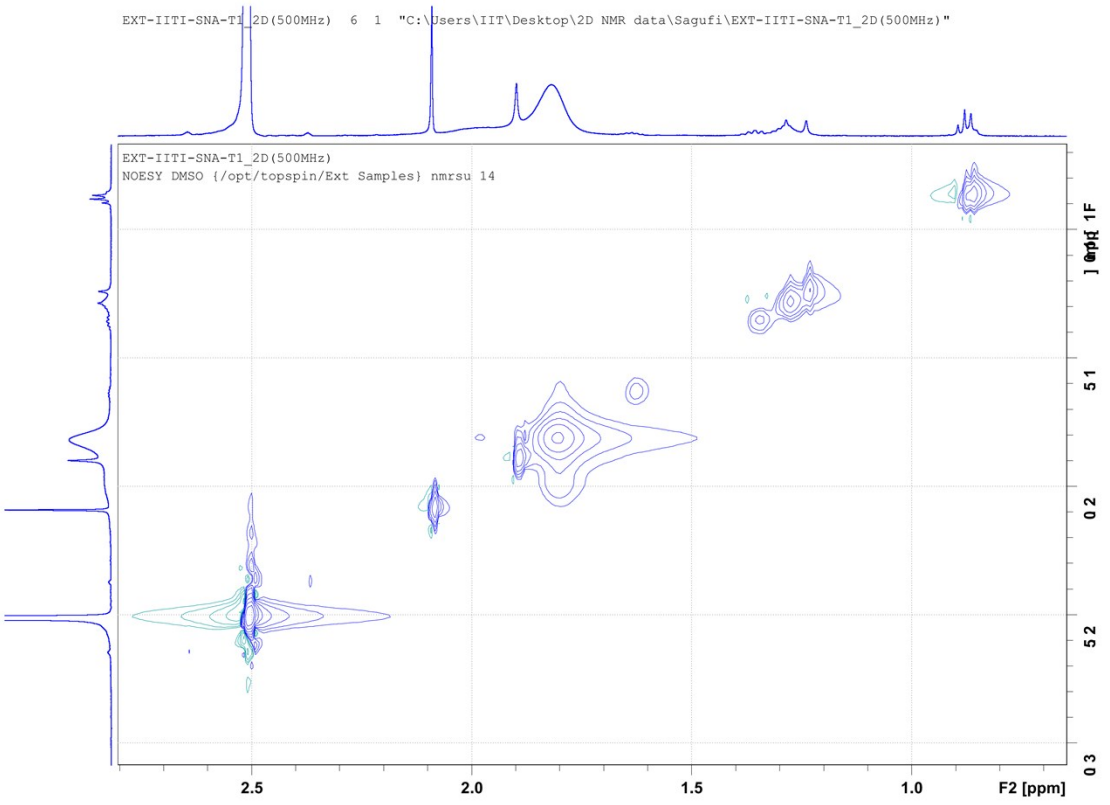

Fig S25. NOESY (DMSO-*d*6, 500MHz) of Complex **1** (Aliphatic region).

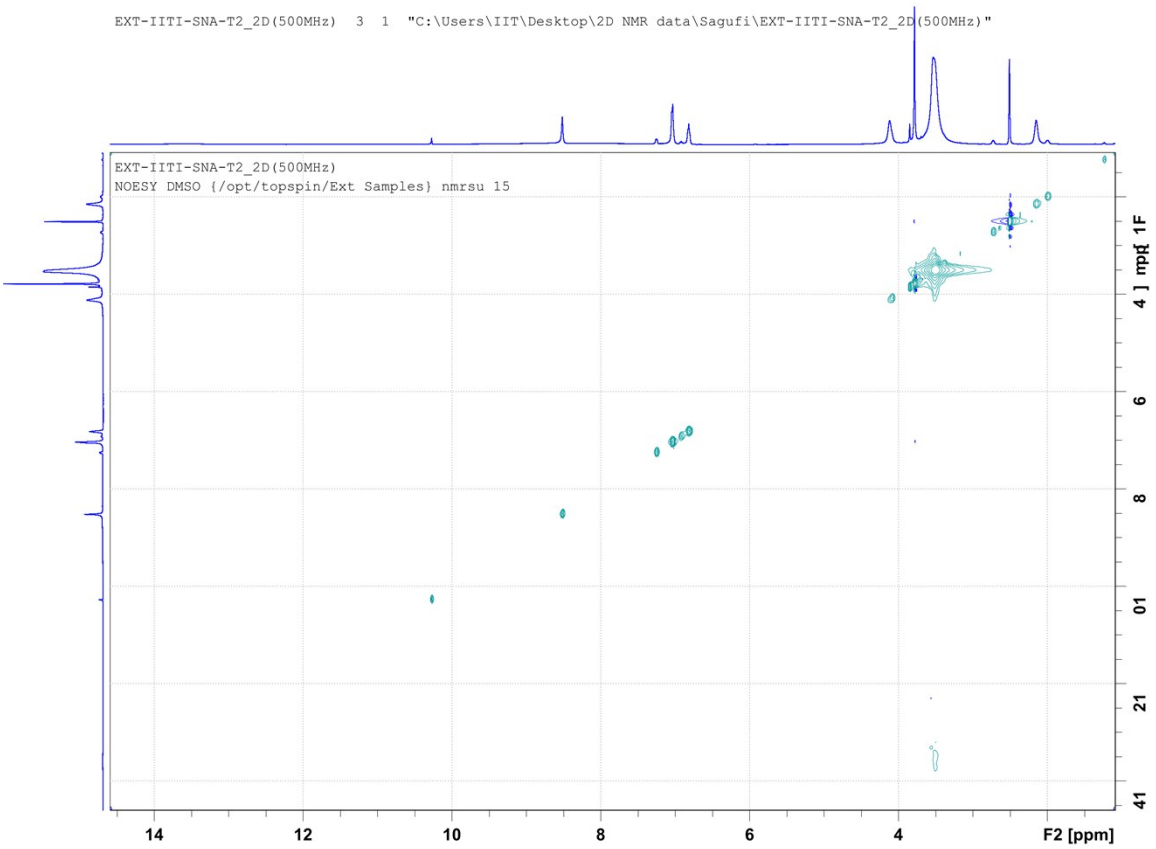

Fig S26. NOESY (DMSO-*d*6, 500MHz) of Complex **2**.

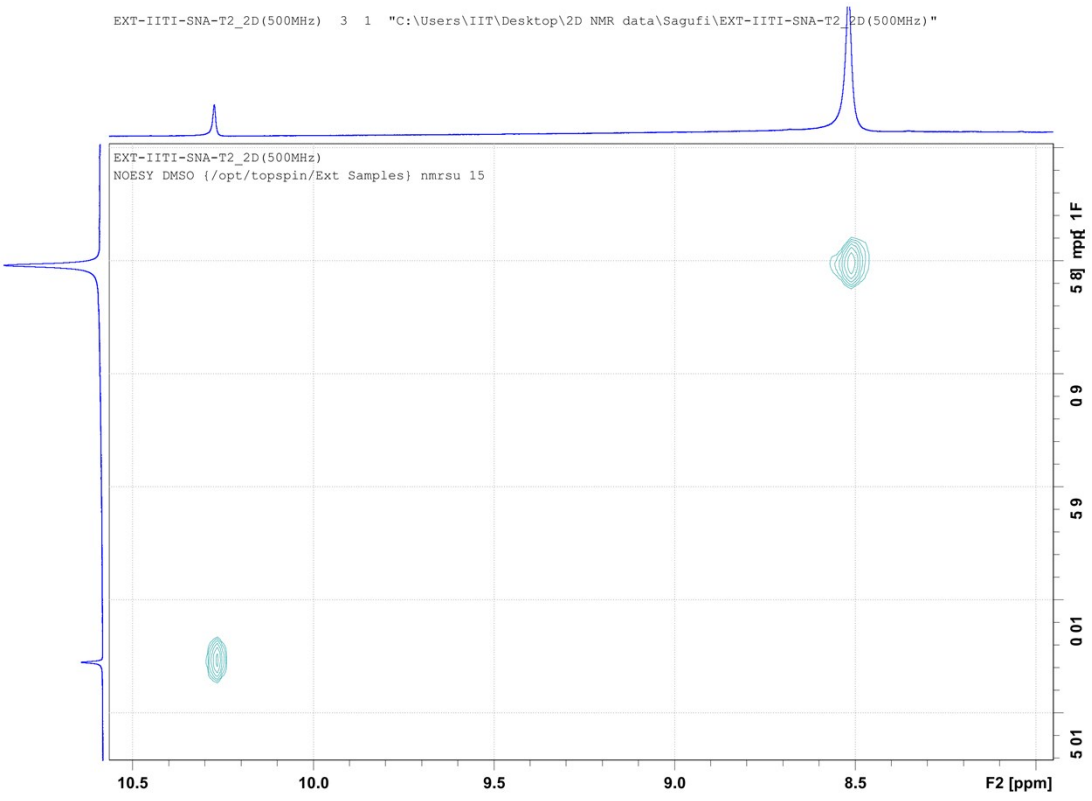

Fig S27. NOESY (DMSO-*d*6, 500MHz) of Complex **2** (Aromatic region).

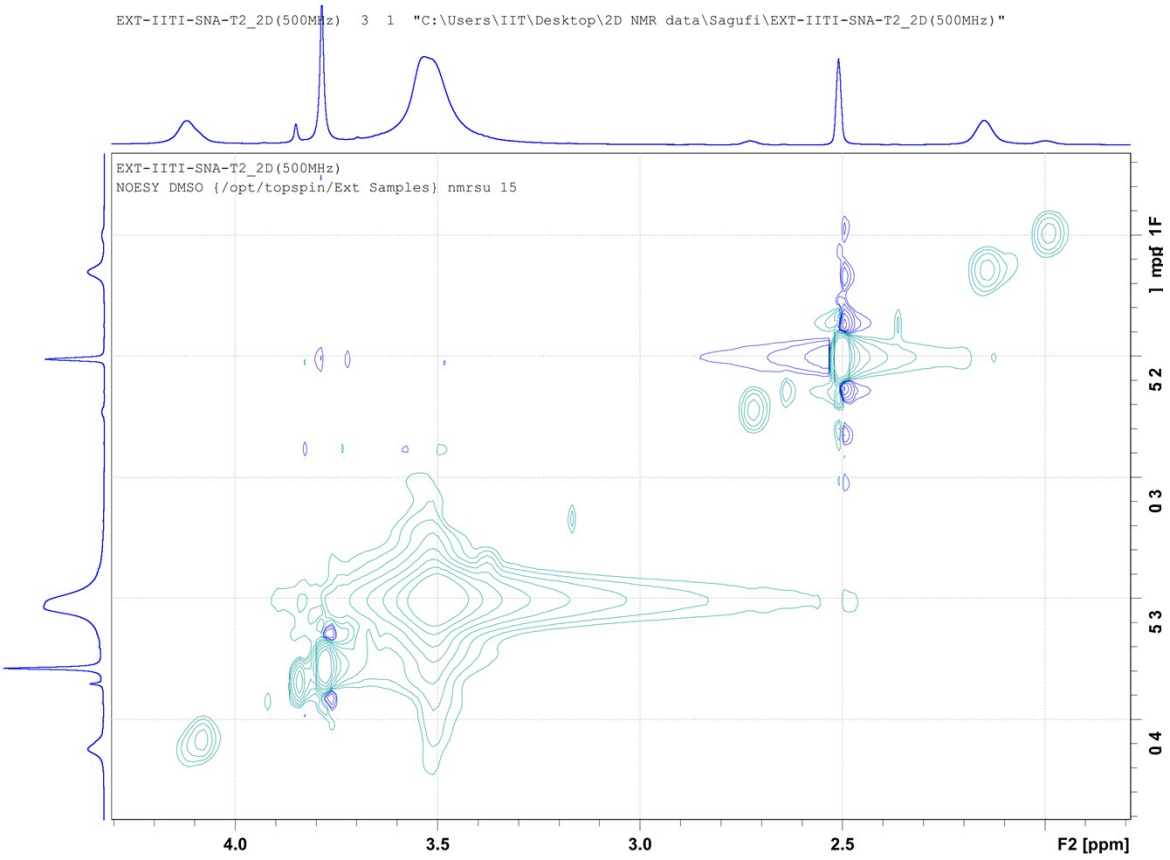

Fig S28. NOESY (DMSO-*d*6, 500MHz) of Complex **2** (Aliphatic region).

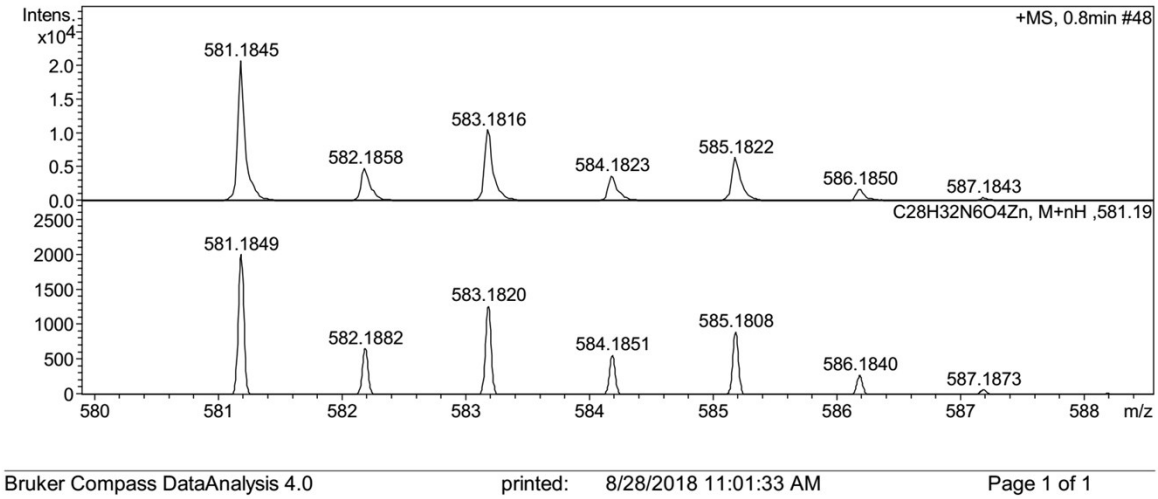

Fig S29. HRMS spectrum of complex **1**.

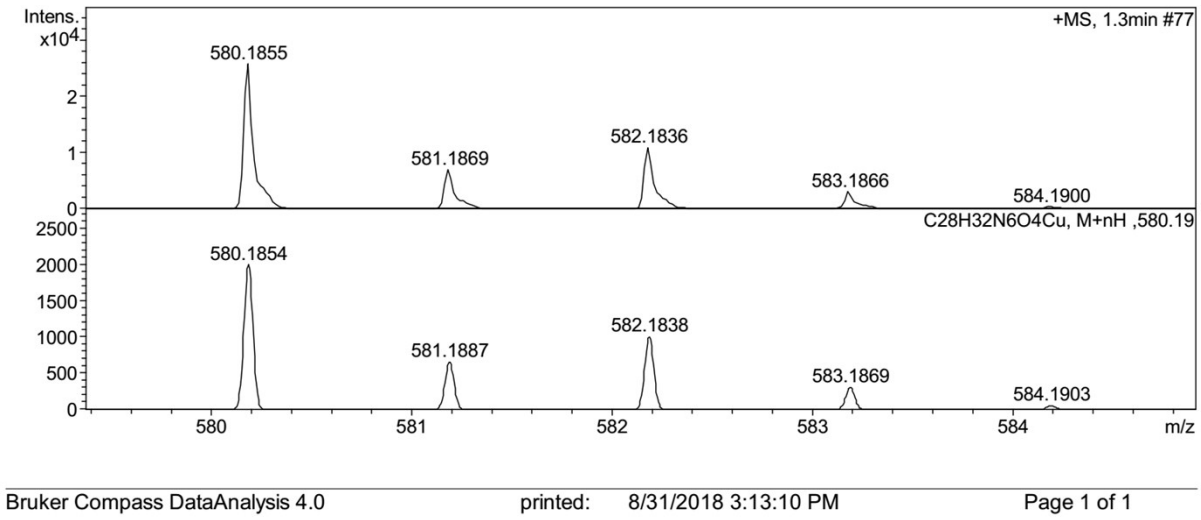

Fig S30. HRMS spectrum of complex **2**.

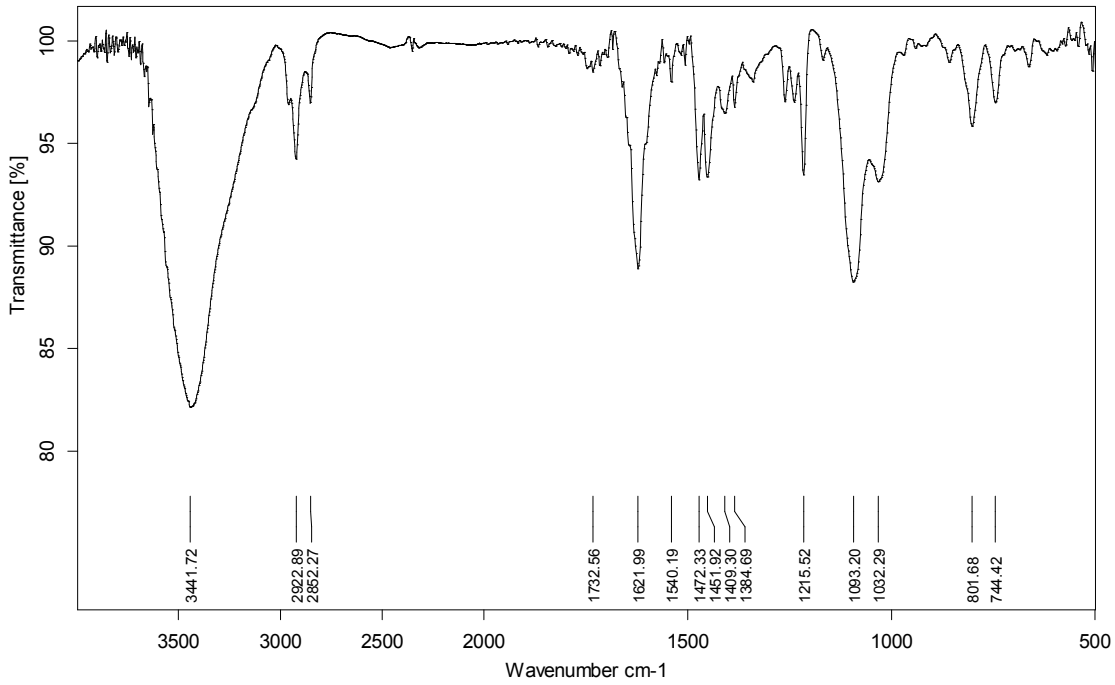

Fig S31. IR Spectrum of complex **1**.

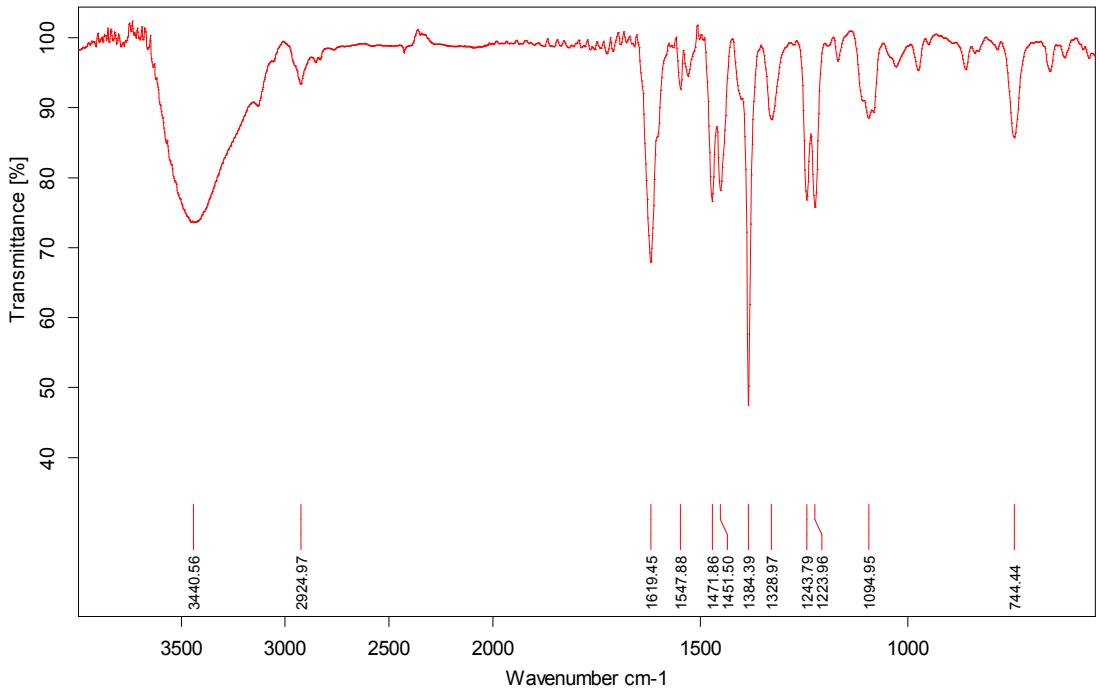

Fig S32. IR Spectrum of complex **2**.

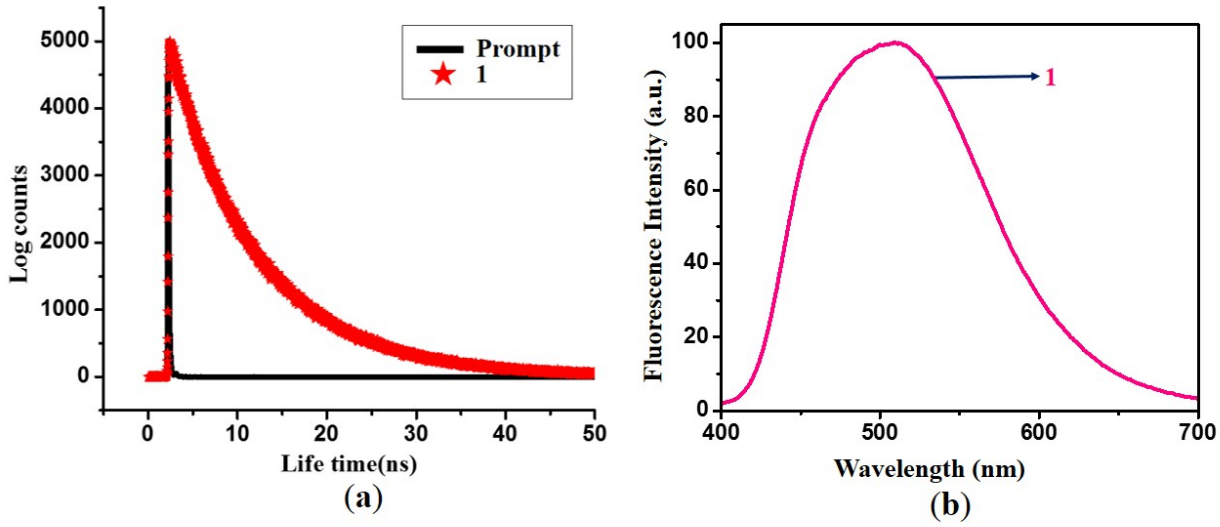

Fig S33. (**a**) Average lifetime measurement of **1** in ACN. (**b**) Fluorescence spectra of **1** in ACN.

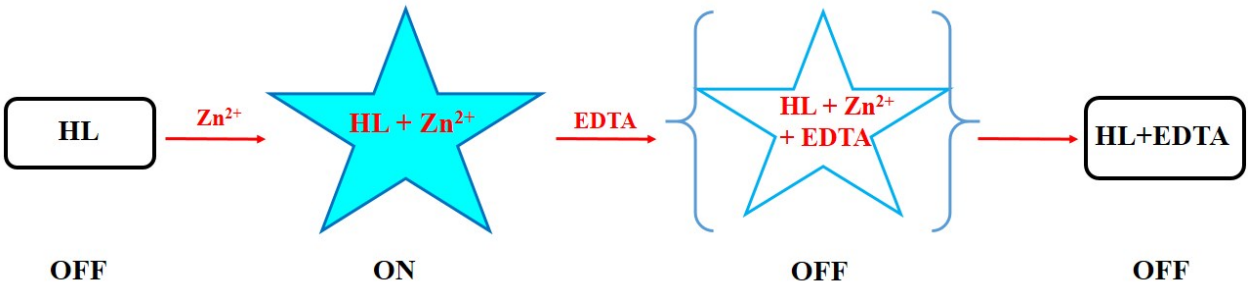

Fig S34. Schematic representation of fluorescence quenching.

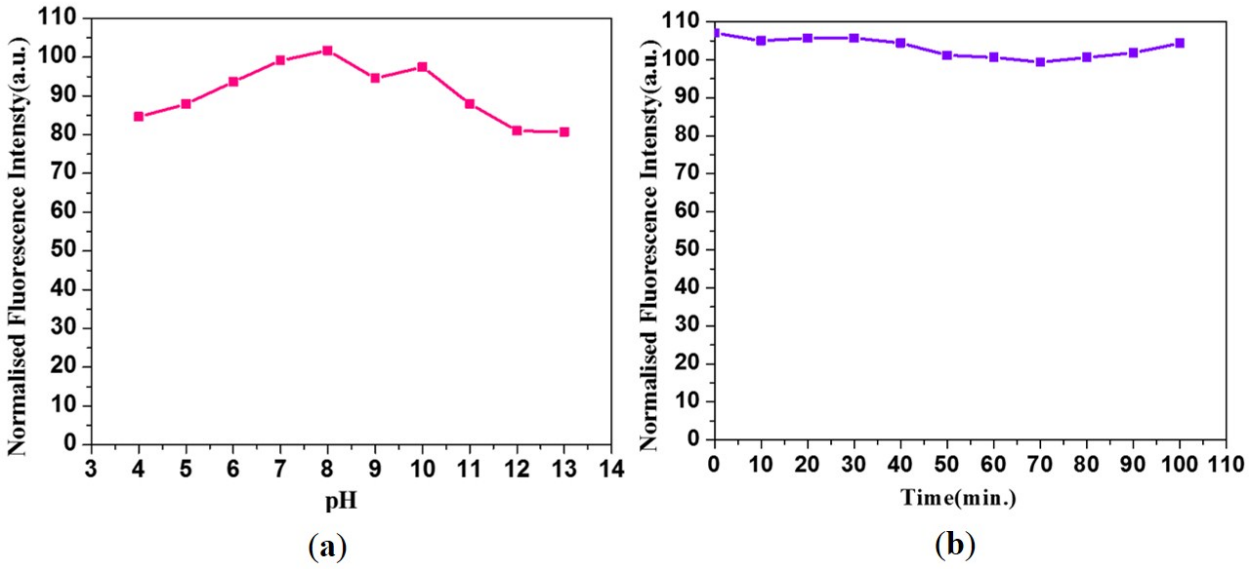

Fig S35. Stability of fluorescence intensity of **1** at (**a**) varied pH, (**b**) varied UV illumination.

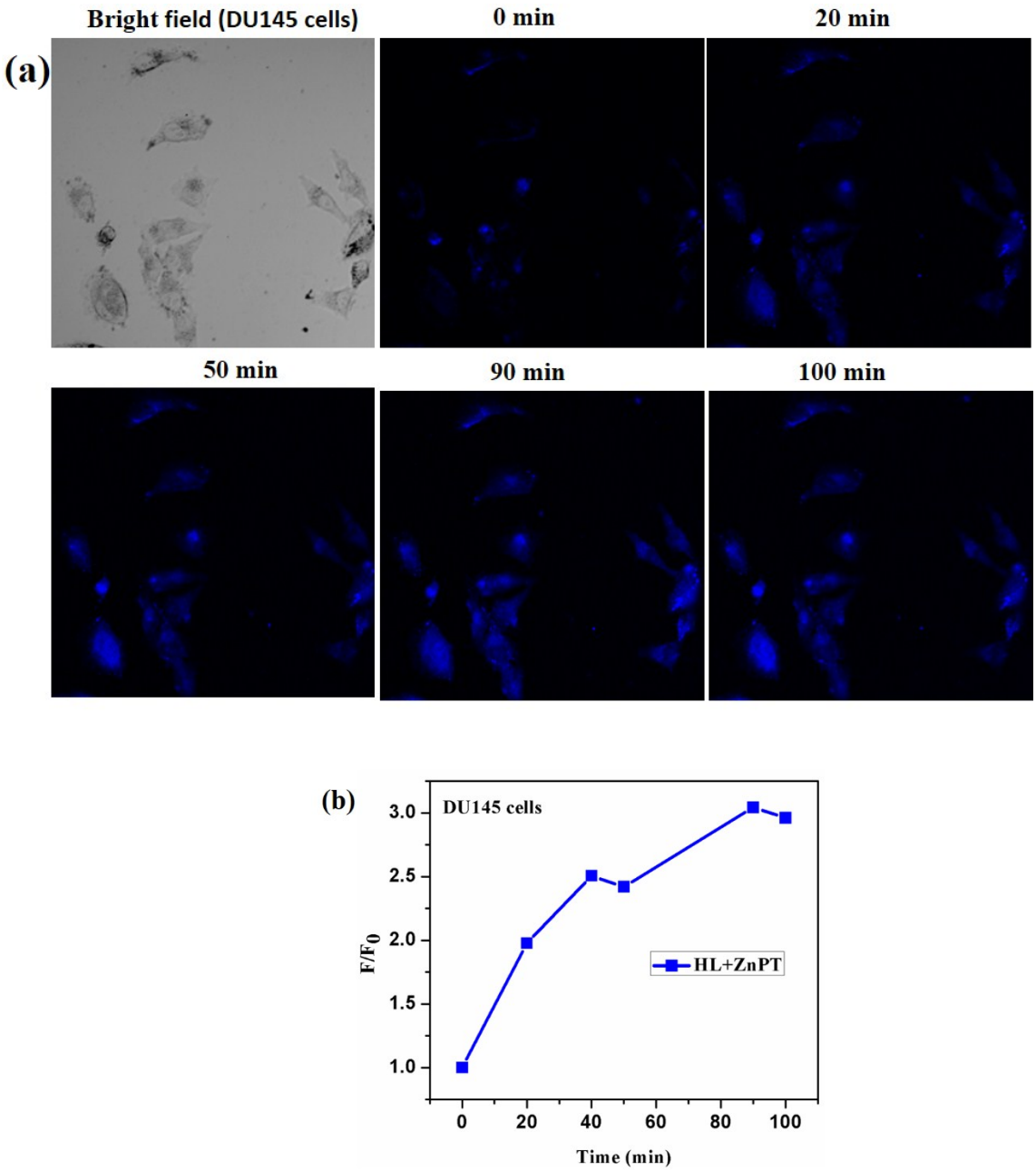

Fig S36. (**a**) DU145 cells pre-incubated with **HL** (25 μM ; 2 h), after washing with PBS, image taken (0 min image) then treated with Zinc pyrithione (ZnPT) without disturbing cells position. Images were captured after different time interval. (**HL** λ_{ex}= 405, λ_{em} = 420–470). (**b**) Quantification of the change in fluorescence signal intensity of **HL** after addition of ZnPT on DU145 cells.

References

1 G. M, Sheldrick, *Acta Cryst*., 2015, **C71**, 3–8.

2 Scientific Computing World., 2002, **63**, 19.